Dynamical mass generation in pseudoquantum electrodynamics with four-fermion interactions

Van Sérgio Alves,[1] Reginaldo O. C. Junior,[2] E. C. Marino,[2] and Leandro O. Nascimento[3,4]

[1]*Faculdade de Física, Universidade Federal do Pará, Avenida Augusto Correa 01, Belém, Pará 66075-110, Brazil*

[2]*Instituto de Física, Universidade Federal do Rio de Janeiro, C.P. 68528, Rio de Janeiro, Rio de Janeiro 21941-972, Brazil*

[3]*International Institute of Physics, Campus Universitário Lagoa Nova, C.P. 1613, Natal, Rio Grande do Norte 59078-970, Brazil*

[4]*Faculdade de Ciências Naturais, Universidade Federal do Pará, C.P. Breves, Pará 68800-000, Brazil*

(Received 4 April 2017; revised manuscript received 6 July 2017; published 7 August 2017)

We describe dynamical symmetry breaking in a system of massless Dirac fermions with both electromagnetic and four-fermion interactions in $(2+1)$ dimensions. The former is described by the pseudo quantum electrodynamics, and the latter is given by the so-called Gross-Neveu action. We apply the Hubbard-Stratonovich transformation and the large-N_f expansion in our model to obtain a Yukawa action. Thereafter, the presence of a symmetry broken phase is inferred from the nonperturbative Schwinger-Dyson equation for the electron propagator. This is the physical solution whenever the fine-structure constant is larger than a critical value $\alpha_c(DN_f)$. In particular, we obtain the critical coupling constant $\alpha_c \approx 0.36$ for $DN_f = 8.$, where $D = 2, 4$ corresponds to the SU(2) and SU(4) cases, respectively, and N_f is the flavor number. Our results show a decreasing of the critical coupling constant in comparison with the case of pure electromagnetic interaction, thus yielding a more favorable scenario for the occurrence of dynamical symmetry breaking. Nevertheless, the number of renormalized masses is not changed by the four-fermion interaction within our approximation. For two-dimensional materials, in application in condensed matter systems, it implies an energy gap at the Dirac points or valleys of the honeycomb lattice.

DOI: 10.1103/PhysRevD.96.034005

I. INTRODUCTION

Two-dimensional quantum field theories are relevant for describing the electronic interactions in thin materials, for instance, graphene and transition metal dichalcogenides [1]. They also have been applied as minimal models for describing some particular features of quantum chromodynamics, in particular, the quark confinement [2]. For condensed matter physics, we may comment on the discovery of topological states of matter, which are described by topological order instead of spontaneous symmetry breaking [3,4].

Having in mind two-dimensional materials, we may separate the interactions into two classes: one due to the electric charge and the other due to microscopic interactions that emerge in these systems, for instance, phonons, impurities, and disorder. The first case is described by pseudo quantum electrodynamics (PQED), the derivation of which has been made in Ref. [5]. The main procedure is to confine the matter current into the plane but to keep photons free to propagate out of this plane. One of the advantages is to recover the usual Coulomb interaction in the plane instead of the logarithmic potential, typical of quantum electrodynamics in $(2+1)$ dimensions (QED3). Several features of PQED have been discussed in the literature [6–13]. In the static limit, the Coulomb interaction renormalizes the Fermi velocity [14] of electrons in graphene, accordingly to the experimental measurements in Ref. [15]. At the neutrality point in graphene, Lorentz symmetry is expected to be recovered. The second kind of interactions is not described by a unique model. In general grounds, it is expected to be given by some electron-electron action.

For graphene, in the absence of external magnetic field and considering the full electromagnetic interaction, the emergence of a quantized valley Hall conductivity at low temperatures has been shown. Essentially, this effect is explained by the dynamical generation of mass in the electronic spectrum, above a certain critical coupling constant α_c [6]. The role of PQED for describing topological states of matter has been discussed in Ref. [16]. In particular, for massive Dirac systems, the existence of an emerging quantum Hall effect has been shown [17]. It is worth it to remember that the Hall conductivity is only defined in the SU(2) representation, where the mass breaks time-reversal symmetry. In the SU(4) representation, dynamical mass generation has been calculated for PQED in both zero [7] and finite [8] temperatures, describing chiral symmetry breaking. Similar results have been obtained for QED3 [18,19] and quantum electrodynamics in (3+1) dimensions (QED4) earlier; see Refs. [2] for a detailed review about these studies. On the other hand, the description of dynamical symmetry breaking in gauge theories with additional four-fermion interactions has been

discussed less [20]. In particular, this case for PQED has not been investigated until now.

In this paper, we calculate the pattern of dynamical mass generation in PQED, including a Gross-Neveu interaction [21] at zero temperature, and both SU(2) and SU(4) representations are discussed. The main goal is to investigate the critical behavior of this more general theory.

The outline of this paper is the following. In Sec. II, we introduce our model within the PQED approach and the usual Gross-Neveu model. In Sec. III, we apply the Hubbard-Stratonovich transformation in the Gross-Neveu model, using the large N_f expansion. In Sec. IV, we calculate the auxiliary and gauge-field propagators in the large-N_f expansion. In Sec. V, we write the Schwinger-Dyson equation for the matter field. In Sec. VI, we calculate the mass function $\Sigma(p)$ in the unquenched-rainbow approach. In Sec. VII, we calculate the physical mass. In Sec. VIII, we summarize and give an outlook for our main results. We also include three Appendixes, where we derive the integral equation to wave function renormalization (see Appendix A), derive the differential equation for the mass function (see Appendix B), and perform numerical tests (see Appendix C).

II. MODEL

We assume that the Dirac electrons will interact through the electromagnetic interaction, which in 2D is described by PQED [5]. Furthermore, we assume a finite four-fermion interaction. The corresponding Lagrangian reads

$$\mathcal{L}=\frac{1}{4}F_{\mu\nu}\left[\frac{2}{\sqrt{-\Box}}\right]F^{\mu\nu}+i\bar{\psi}_a\partial\!\!\!/\psi_a+j^\mu A_\mu-\frac{G}{2}(\bar{\psi}_a\psi_a)^2, \quad (1)$$

where $j^\mu = e\bar{\psi}_a\gamma^\mu\psi_a$ is the matter current. ψ_a is a four-component Dirac field; $\bar{\psi}_a=\psi_a^\dagger\gamma^0$ is its adjoint; $F_{\mu\nu}$ is the usual field intensity tensor of the U(1) gauge field A_μ, which intermediates the electromagnetic interaction in 2D (pseudo electromagnetic field); γ^μ are rank-2 Dirac matrices; and $a=1,\ldots,N_f$ is a flavor index. The coupling constant $e^2=4\pi\alpha$ is conveniently written in terms of α, the fine-structure constant in natural units. G is the coupling constant related to the four-fermion interaction, i.e., the Gross-Neveu interaction. The dimension of G is the inverse of energy, namely, $[G]=[M]^{-1}$. Without four-fermion interactions ($G=0$), an SU(4) version of this model has been recently used to study dynamical gap generation and chiral symmetry breaking in graphene [7]. For $\alpha=0$, Eq. (1) is the Gross-Neveu model.

The bare gauge-field propagator, in the Landau gauge, reads

$$G_{0,\mu\nu}(p)=\frac{P_{\mu\nu}}{2\sqrt{p^2}}, \quad (2)$$

where $P_{\mu\nu}=\delta_{\mu\nu}-p_\mu p_\nu/p^2$ is the transversal operator. The bare fermion propagator is

$$S_{0,F}(p)=\frac{1}{\gamma^\mu p_\mu}. \quad (3)$$

Next, we introduce an auxiliary field in order to transform the action from the four-fermion interaction to a Yukawa action. This transformation is also known as the Hubbard-Stratonovich transformation.

III. AUXILIARY FIELD

Let us first consider the fermionic terms in Eq. (1), i.e., the Gross-Neveu action $\mathcal{L}_{\rm GN}$, given by

$$\mathcal{L}_{\rm GN}=i\bar{\psi}_a\partial\!\!\!/\psi_a-\frac{G}{2}(\bar{\psi}_a\psi_a)^2. \quad (4)$$

In the large-N_f expansion, we define a new coupling constant $g=GN_f$, such that g is meant to be fixed for N_f large. Next, we introduce an auxiliary field $\varphi(x)$ in Eq. (4) in order to obtain a three-linear vertex interaction. Therefore, we perform the transformation

$$\mathcal{L}_{\rm GN}\to\mathcal{L}_{\rm GN}+\frac{1}{2g}\left(\varphi-\frac{g}{\sqrt{N_f}}\bar{\psi}_a\psi_a\right)^2, \quad (5)$$

which gives the transformed action

$$\mathcal{L}_{GN}=i\bar{\psi}_a\partial\!\!\!/\psi_a-\frac{\varphi}{\sqrt{N_f}}\bar{\psi}_a\psi_a+\frac{\varphi^2}{2g}. \quad (6)$$

It is straightforward, from the minimal principle for the auxiliary field $\delta\mathcal{L}/\delta\varphi=0$, to show that

$$\varphi=\frac{g}{\sqrt{N_f}}\bar{\psi}_a\psi_a, \quad (7)$$

proving that the transformation in Eq. (5) does not change the dynamics of the Gross-Neveu model in Eq. (4) [see Eq. (5)]. Here, it is more convenient to consider Eq. (6). The propagator of the auxiliary field is given by

$$\Delta_{0,\varphi}=\frac{1}{1/g}, \quad (8)$$

which clearly has no dynamics at bare level. Within this approach, Eq. (1) becomes

$$\mathcal{L}=\frac{1}{4}F_{\mu\nu}\left[\frac{2}{\sqrt{-\Box}}\right]F^{\mu\nu}+i\bar{\psi}_a\partial\!\!\!/\psi_a+j_a^\mu A_\mu -\frac{\varphi}{\sqrt{N_f}}\bar{\psi}_a\psi_a+\frac{\varphi^2}{2g}. \quad (9)$$

The main advantage of including the auxiliary field is that we have to deal with a three-linear vertex instead of a four-linear vertex. Next, we would like to calculate the

possibility of dynamical mass generation due to interactions. The natural method to investigate such phenomena is the Schwinger-Dyson equation for the electron propagator, which yields nontrivial results at large coupling constants. This is a system of coupled integral equations, connecting all of the full propagators in the theory. To obtain an analytical solution for the electron, we must approximate both the gauge and scalar propagators. The easiest approach would be to consider only the bare propagators. Here, nevertheless, we choose to apply the large-N_f expansion, which allows us to include quantum fluctuations in these propagators.

IV. LARGE-N_f EXPANSION FOR BOTH φ AND A_μ

In this section, we apply the large-N_f expansion in order to obtain the full propagators of the auxiliary and the gauge fields. For the auxiliary field $\varphi(x)$, we have

$$\Delta_\varphi^{-1} = \Delta_{0,\varphi}^{-1} - \Pi(p), \tag{10}$$

where Δ_φ^{-1} is the full propagator. $\Pi(p)$ is the quantum correction due to interaction with the matter field. This is given by the fermionic loop, namely,

$$\Pi(p) = -\mathrm{Tr}\int \frac{d^3k}{(2\pi)^3} S_F(p-k)S_F(k). \tag{11}$$

In Eq. (11), $S_F(p)$ is the full electron propagator. Because we do not know this propagator, we use the bare electron propagator in Eq. (3) in order to find an analytical result for Δ_φ. Thereafter a standard calculation, we find $\Pi(p) = \sqrt{p^2}x_0$, with $x_0 = D/16$ ($D = 2, 4$ is the rank of the Dirac matrices), and

$$\Delta_\varphi(p) = \frac{1}{1/g + \sqrt{p^2}x_0}. \tag{12}$$

Remarkably, the self-energy of the auxiliary field yields a nontrivial dynamics for the propagator of the auxiliary field. This shall have an important effect on the criticality of our model; see Sec. VI.

Next, we apply the very same set of approximations for the gauge field. In this case, the Schwinger-Dyson equation reads

$$G_{\mu\nu}^{-1} = G_{0,\mu\nu}^{-1} - \Pi_{\mu\nu}, \tag{13}$$

where $G_{\mu\nu}$ is the full propagator of the gauge field and $\Pi_{\mu\nu}$ is the vacuum polarization tensor, which has been calculated in Ref. [22]. From Eq. (13), we have

$$G_{\mu\nu} = G_{0,\mu\alpha}[\delta_\nu^\alpha - \Pi^{\alpha\beta}G_{0,\beta\nu}]^{-1}. \tag{14}$$

The vacuum polarization tensor may be decomposed into

$$\Pi_{\mu\nu} = e^2\Pi_1 P_{\mu\nu} + e^2\Pi_2\epsilon_{\mu\nu\alpha}p^\alpha, \tag{15}$$

where Π_1 and Π_2 are known functions [22]. Using Eqs. (2) and (15) in Eq. (14), we find

$$G_{\mu\nu} = \Delta_1 P_{\mu\nu} + \Delta_2\epsilon_{\mu\nu\alpha}p^\alpha, \tag{16}$$

where

$$\Delta_1 = \frac{2\sqrt{p^2} - e^2\Pi_1}{(2\sqrt{p^2} - e^2\Pi_1)^2 + e^4p^2\Pi_2^2} \tag{17}$$

and

$$\Delta_2 = \frac{e^2\Pi_2}{(2\sqrt{p^2} - e^2\Pi_1)^2 + e^4p^2\Pi_2^2}. \tag{18}$$

From the trace properties of the Dirac matrices, it is possible to show that the term Δ_2 does not contribute for dynamical symmetry breaking. Indeed, one may keep this term in the gauge-field propagator, and the result shall be the same at the end of the calculations. On the other hand, assuming a small electric charge and using $\Pi_1 = -pN_fD/32$ [22], we have

$$G_{\mu\nu}(p) = \frac{P_{\mu\nu}}{\sqrt{p^2}(2 + \frac{\lambda D}{32})}, \tag{19}$$

where $\lambda = e^2N_f$ is the coupling constant in the large-N_f expansion [7]. In Eq. (19), $D = 2, 4$ are the two possible representations of the Dirac field, which has two or four components, respectively.

Next, we use the propagators in Eqs. (19) and (12) to calculate the full electron propagator $S_F(p)$. Thereafter, we shall use this function to obtain the dynamically generated masses.

V. SCHWINGER-DYSON EQUATION OF THE MATTER FIELD

The Schwinger-Dyson equation for the electron reads [2]

$$S_F^{-1}(p) = S_{0F}^{-1}(p) - \Xi(p), \tag{20}$$

where S_{0F} and S_F are the free- and interacting-electron propagators, respectively. $\Xi(p)$ is the electron self-energy, which has two contributions $\Xi(p) = \Xi^\alpha(p) + \Xi^g(p)$, where $\Xi^\alpha(p)$ and $\Xi^g(p)$ are the electron self-energies due to the electromagnetic and four-fermion interactions, respectively. The diagrammatic representation is shown in Fig. 1. The electron self-energies are given by

$$\Xi^\alpha(p) = \frac{\lambda}{N_f}\int \frac{d^3k}{(2\pi)^3}\gamma^\mu S_F(k)\gamma^\nu G_{\mu\nu}(p-k) \tag{21}$$

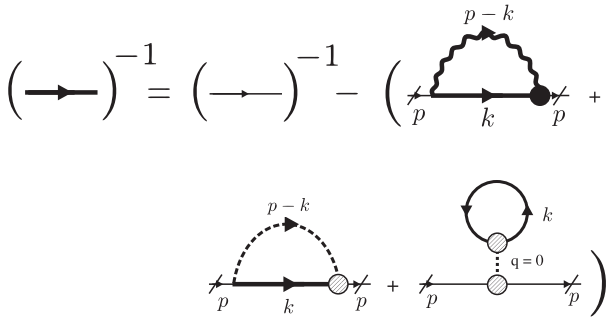

FIG. 1. Diagrammatic representation of Eq. (20). The bold lines are the full electron propagator, and the thin line is the free electron propagator. The dashed line is the auxiliary-field propagator, and the wavelike line is the gauge-field propagator, both of them in the large-N_f expansion. The cross-hatched circle is the full vertex, related to the Yukawa interaction. The black circle is the full vertex, related to the electromagnetic interaction. Note that we have neglected all corrections to the vertex functions, which is called the rainbow approach.

and

$$\Xi^g(p) = \frac{1}{N_f}\int \frac{d^3k}{(2\pi)^3}\Delta_\varphi(p-k)S_F(k) + \\ - \Delta_\varphi(0)\mathrm{Tr}\int \frac{d^3k}{(2\pi)^3}S_F(k). \tag{22}$$

To obtain analytical solutions of the Schwinger-Dyson equation, it is convenient to rewrite the full fermion propagator as [19]

$$S_F^{-1}(p) = p_\mu\gamma^\mu A(p) - \Sigma(p), \tag{23}$$

where $A(p)$ is usually called the wave function renormalization and $\Sigma(p)$ is the mass function. Inserting Eq. (23) into Eq. (20), we obtain the integral equation

$$\Sigma(p) = \frac{2\lambda}{N_f}\int \frac{d^3k}{(2\pi)^3}\frac{\Sigma(k)}{A^2(k)k^2+\Sigma^2(k)}\frac{1}{\sqrt{(p-k)^2}(2+\frac{\lambda D}{32})} \\ + \frac{1}{N_f}\int \frac{d^3k}{(2\pi)^3}\frac{\Delta_\varphi(p-k)\Sigma(k)}{A^2(k)k^2+\Sigma^2(k)} \\ - \Delta_\varphi(0)\int \frac{d^3k}{(2\pi)^3}\frac{\mathrm{Tr}\Sigma(k)}{A^2(k)k^2+\Sigma^2(k)}. \tag{24}$$

From now on, we shall consider $A(p)\approx 1$; see Appendix A and Appendix C for more details.

VI. DYNAMICAL SOLUTION FOR $\Sigma(p)$

The third term on the rhs of Eq. (24) does not change momentum. Hence, we focus on the dynamical solutions of the mass function driven by a kernel with p dependence. This regime is obtained when both gauge and auxiliary propagators change momentum with the electron propagator,

$$\Sigma(p) = \frac{2\lambda}{N_f}\int \frac{d^3k}{(2\pi)^3}\frac{\Sigma(k)}{k^2+\Sigma^2(k)}\frac{1}{\sqrt{(p-k)^2}(2+\frac{\lambda D}{32})} \\ + \frac{1}{N_f}\int \frac{d^3k}{(2\pi)^3}\frac{\Sigma(k)}{k^2+\Sigma^2(k)}\frac{1}{1/g+\sqrt{(p-k)^2}x_0}. \tag{25}$$

We use spherical coordinates $d^3k = k^2dk\sin\theta d\theta d\phi$, and hence the polar integral gives a factor 2π. Next, we solve the angular integral in both the first and second terms on the rhs of Eq. (25).

Let us first consider only the integral which is proportional do λ, i.e., the first term of the rhs of Eq. (25). By defining $u \equiv p^2+k^2-2pk\cos\theta$ and changing the integral variable into u, we find

$$\frac{2\lambda}{4\pi^2 N_f}\frac{1}{(2+\frac{\lambda D}{32})}\int_0^\infty \frac{k^2dk\Sigma(k)}{k^2+\Sigma^2(k)}\left(\frac{|p+k|-|p-k|}{pk}\right). \tag{26}$$

For the second term on the rhs, the same procedure yields

$$\frac{1}{4\pi^2 x_0 N_f p}\int_0^\infty \frac{kdk\Sigma(k)}{k^2+\Sigma^2(k)}\left\{[|p+k|-|p-k| \right. \\ \left. -\frac{1}{x_0 g}\ln\left[\frac{(x_0g)^{-1}+|p-k|}{(x_0g)^{-1}+|p+k|}\right]\right\}. \tag{27}$$

Therefore, the integral equation becomes

$$\Sigma(p) = \frac{C_2}{p}\int_0^\infty \frac{kdk\Sigma(k)}{k^2+\Sigma^2(k)}\ln\left[\frac{(x_0g)^{-1}+|p-k|}{(x_0g)^{-1}+|p+k|}\right] \\ + \frac{C_1}{p}\int_0^\infty \frac{kdk\Sigma(k)}{k^2+\Sigma^2(k)}(|p+k|-|p-k|), \tag{28}$$

where

$$C_1 = \frac{2\lambda}{4\pi^2 N_f(2+\lambda D/32)} + \frac{g}{N_f(gx_0)4\pi^2}, \tag{29}$$

and

$$C_2 = -\frac{g}{N_f(gx_0)^2 4\pi^2}. \tag{30}$$

Equation (28) is a nonlinear integral equation for $\Sigma(p)$. We may obtain numerical solutions; see Appendix B for more details. Nevertheless, it is useful to find some analytical solution, in particular, to calculate critical

parameters. To do so, we must to convert Eq. (28) into a differential equation. First, it is convenient to obtain a scale-invariant integral equation (without any dimensional parameter). Indeed, by defining $\Sigma(p)\equiv f(pg)/g$, $x\equiv gp$, and $y\equiv gk$, we find

$$f(x)=\frac{gC_2}{x}\int_0^\infty \frac{ydyf(y)}{y^2+f^2(y)}\ln\left[\frac{(x_0)^{-1}+|x-y|}{(x_0)^{-1}+|x+y|}\right] + \frac{C_1}{x}\int_0^\infty \frac{ydyf(y)}{y^2+f^2(y)}(|x+y|-|x-y|). \tag{31}$$

From Eq. (31), we have the functional dependence of the mass function on the momentum and other parameters: $\Sigma(p)=g^{-1}f(gp)$. This result shows that the critical values of λ and N_f are related. The dimensional coupling constant g only changes the scale of the external momentum p. This result is exact. Indeed, with $g=0$, PQED with a massless Dirac fermion is scale invariant and has a critical coupling constant λ_c or a critical number of flavors N_c [7].

We may obtain analytical solutions by introducing an ultraviolet cutoff Λ, thus converting Eq. (31) into a differential equation in the linearized regime, where $x\gg f(x)$ (see Appendix B). In this case, we have

$$\frac{d}{dx}\left(x^2\frac{df(x)}{dx}\right)+\frac{N_c}{4N_f}f(x)=0, \tag{32}$$

where

$$N_c(\lambda)=\frac{2}{\pi^2}\left(\frac{2\lambda}{2+\lambda D/32}+\frac{16}{D}\right) \tag{33}$$

is the critical number of flavors. The mass function is nontrivial only if $N_f\le N_c$ (similar to QED3 with $G=0$ [18]). We shall prove this after we calculate the physical masses.

The solutions of Euler's differential equation are

$$f(x)=A_+x^{a_+}+A_-x^{a_-}, \tag{34}$$

where $a_\pm=-1/2\pm 1/2\sqrt{1-N_c/N_f}$ and A_+ and A_- are arbitrary constants. Hence, the real part of the solution is

$$\mathrm{Re}\{f(x)\}=\frac{F}{\sqrt{x}}\cos[\gamma\ln x+\theta_0], \tag{35}$$

where F and θ_0 are arbitrary real constants, without loss of generality, given by $F=2\sqrt{A_+A_-}$ and $\theta_0=\tan^{-1}[(i(A_+-A_-))/(A_+A_-)]$. Indeed, it is straightforward to check that it satisfies Euler's differential equation. Using Eq. (35) in Eq. (32), we find that the real constant γ is given by

$$\gamma=\frac{1}{2}\sqrt{\frac{N_c}{N_f}-1}. \tag{36}$$

This is the main parameter for describing dynamical mass generation; i.e., whether γ is real, we have real generated masses [see Eq. (46) in Sec. VII].

Next, we compare this criticality with some known results for QED3 [18] and PQED [7] without four-fermion interaction. From Eq. (33) and $\lambda=4\pi\alpha N_f$, we have

$$N_c(\alpha)=\frac{2}{\pi^2}\left(\frac{8\pi\alpha N_f}{2+\pi\alpha N_f D/8}+\frac{16}{D}\right). \tag{37}$$

Comparison with Eq. (44) in Ref. [6] shows that the second term on the right-hand side of Eq. (37), namely, $32/(\pi^2 D)=2/(\pi^2 x_0)$, is the nontrivial contribution of the Yukawa action; i.e., it is the consequence of $g\neq 0$ in our model. Although g does not explicit appear in γ, this term is a consequence of the quantum corrections of the scalar-field propagator, which is dependent on x_0; see Eq. (12). It is not possible that g changes γ, because of scale invariance, and hence the critical point is only dependent on α within our approach.

From Eq. (37), we find $0.81\le N_c(\alpha)\le 4.05$ for $D=4$ and $1.61\le N_c(\alpha)\le 8.10$ for $D=2$, where the lower and upper limits have been calculated from the $\alpha\to 0$ and $\alpha\to\infty$ cases, respectively. For QED3, the critical number is $N_c^{\mathrm{QED3}}=32/\pi^2\approx 3.24$ [18]. For graphene, the critical point N_c may be modified by a substrate or by renormalization of the Fermi velocity, because $\alpha=e^2/(4\pi\epsilon v_F)$, where ϵ and v_F are the dielectric constant and Fermi velocity, respectively.

It is interesting to obtain a critical fine-structure constant α_c. Using Eq. (33) in Eq. (36), we have

$$\gamma=\frac{1}{2}\sqrt{\frac{2}{\pi^2 N_f}\left(\frac{2\lambda}{2+\lambda D/32}+\frac{16}{D}\right)-1}. \tag{38}$$

We define a λ_c such that for $\lambda\ge\lambda_c$ the factor γ is real, and hence the mass function exists. From Eq. (38), we obtain

$$\frac{2}{\pi^2 N_f}\left(\frac{2\lambda_c}{2+\lambda_c D/32}+\frac{16}{D}\right)=1. \tag{39}$$

Solving Eq. (39) for λ_c, we have

$$\lambda_c=\left(\frac{64}{D}\right)\left(\frac{32-DN_f\pi^2}{DN_f\pi^2-160}\right). \tag{40}$$

Furthermore, using $4\pi\alpha_c N_f=\lambda_c$, we find

$$\alpha_c = \frac{16\pi(\frac{32}{\pi^2 DN_f} - 1)}{DN_f\pi^2 - 160}. \tag{41}$$

Note that γ is real for $\alpha \geq \alpha_c$ because the quantity between parentheses in Eq. (38) is monotonically increasing. Equation (41) shows that the critical constant is a function of DN_f. It precisely shows that the dynamical mass generation is independent on the parameter D. Let us clarify this result. Assume we are in a representation $D = 2$ with $N_f = 4$, as is usually the case for graphene. $N_f = 4$ describes the two spins $\uparrow, \downarrow$ and the two valleys K and K' (internal degrees of freedom). We perform the same calculations in the other representation $D = 4$, hence decreasing the flavor number to $N_f = 2$ (only spins or valleys). It follows that $DN_f = 8$ for both cases; therefore, $\alpha_c \approx 0.36$ is obtained independently of the representation. Furthermore, because this result is much less than $\alpha_c = 1.02$ with $G = 0$ [6], we conclude that the presence of some other microscopic interaction is likely to favor the phase with mass generation, even if the latter is weak.

VII. PHYSICAL MASS M_{ph}

A key ingredient for describing topological states of matter is the opening and closing of an energy gap at the Dirac points, which breaks some discrete symmetry. In other words, the transition from a massless to a massive Dirac theory changes the topological invariant of the model, which is given by the Chern number for two-dimensional materials [23]. Here, because we have calculated the mass function $\Sigma(p)$, we may obtain the physical masses of the theory. This is given by $\Sigma(p) = g^{-1}f(gp)$; see Sec. VI. On the other hand, $f(gp)$ is given by Eq. (35) with the critical point in Eq. (33).

The renormalized spectrum reads $E_{\pm}(\mathbf{p}) = \pm\sqrt{\mathbf{p}^2 + m_{\mathrm{ph}}^2}$, where $2|m_{\mathrm{ph}}|$ is the energy gap at the Dirac point $\mathbf{p} = 0$. By making a Taylor expansion around m_{ph}, the mass function reads

$$\sum(p) = \sum(p = m_{\mathrm{ph}}) + (\gamma^\mu p_\mu - m_{\mathrm{ph}})\frac{\partial\sum(p)}{\partial p}\bigg|_{p=m_{\mathrm{ph}}} + \ldots, \tag{42}$$

and imposing

$$\Sigma(p = m_{\mathrm{ph}}) = m_{\mathrm{ph}}, \tag{43}$$

we may write the full fermion propagator as

$$\begin{aligned} S_F(p) &= \frac{1}{\gamma^\mu p_\mu - \Sigma(p)} \\ &= \frac{1}{(\gamma^\mu p_\mu - m_{\mathrm{ph}})(1 - \frac{\partial\sum(p)}{\partial p}|_{p=m_{\mathrm{ph}}} + \cdots)} \\ &= \frac{\gamma^\mu p_\mu + m_{\mathrm{ph}}}{(p^2 - m_{\mathrm{ph}}^2)(1 - \frac{\partial\sum(p)}{\partial p}|_{p=m_{\mathrm{ph}}} + \cdots)}. \end{aligned} \tag{44}$$

We see that m_{ph} is the pole of the full electron propagator at zero momentum, hence, it is the physical mass. Note that the condition for calculating this is given by Eq. (43), which applies only the real part of the self-energy in Eq. (35). Using $g\Sigma(p) = f(gp)$ (for the real parts), we have

$$g\Sigma(p) = \frac{F}{\sqrt{gp}}\cos[\gamma\ln(gp) + \theta_0]. \tag{45}$$

Next, we use Eq. (43) to calculate m_{ph}. We choose $\theta_0 = 0$ and $F = 1$, without loss of generality. Therefore, using Eq. (45) at $p = m_{\mathrm{ph}}$ and defining $-z \equiv \gamma\ln(gm_{\mathrm{ph}})$, we have

$$m_{\mathrm{ph}} = g^{-1}\exp\left(-\frac{z}{\gamma}\right), \tag{46}$$

where z are solutions of the transcendental equation

$$\exp\left(-\frac{3z}{2\gamma}\right) = \cos z. \tag{47}$$

Note that g^{-1} is the natural cutoff for the theory. For $\alpha \to \alpha_c$ and $\gamma \approx 0$, Eq. (47) gives $z \to z_n = (2n+1)\pi/2$ with an n integer. Therefore, there exists a quantized set of physical masses m_{ph}^n. In Ref. [6], the authors have performed the same calculation for $g = 0$ with the cutoff given by the inverse of the lattice parameter. In this case, it has been shown that the quantized set of masses implies an interaction-driven quantum valley Hall effect for graphene. The unique condition for such a new effect is the generation of the dynamical masses, which breaks time-reversal symmetry in the SU(2) representation [6]. Here, we go further by proving that microscopic interactions, given by a Yukawa action, do not cancel the quantum valley Hall effect. This is not surprising in the view of topological insulator theory because it is well known that the quantum Hall effect experimentally occurs in the presence of impurities or electron-phonon interactions. Indeed, the Yukawa action effectively describes electron-phonon interaction at low energies for graphene; see Ref. [24].

VIII. SUMMARY AND OUTLOOK

We have described the dynamical symmetry breaking in a two-dimensional system, consisting of massless Dirac fermions with two types of interactions. One is the

electromagnetic interaction, described by the PQED approach, and the other is, essentially, a Yukawa action, which originates from some microscopic physical effect, such as electron-phonon interaction. This seems to be case for honeycomb systems at low energies; see Ref. [24] for the case of graphene.

We consider the zero-temperature case at both SU(2) and SU(4) representations, where parity and chiral symmetries are broken in the massive phase, respectively. We show that the critical coupling constant is dependent on the product DNf_f. For graphene, we have $DN_f = 8$ for both SU(2) and SU(4) representations, because the flavor number in the SU(4) case ($N_f = 2$) is half of the flavor number in the SU(2) representation ($N_f = 4$). It is shown that for $DN_f = 8$ the critical coupling constant is $\alpha_c \approx 0.36$. Hence, the presence of some microscopic interaction is likely to improve the possibility of generating a mass in the electronic spectrum. The mass function of the matter field has been calculated from the Schwinger-Dyson equations, using the large-N_f expansion for both the gauge and scalar fields. This is called the unquenched-rainbow approximation in literature. Numerical results show that our analytical approximations are in good agreement with the full integral equation. Furthermore, we have shown that Yukawa interaction does not change the quantized feature of the energy levels, which have been calculated in Ref. [6] for the case of pure PQED.

Note that we lost gauge invariance in the rainbow approximation, which implies a bare vertex for both electromagnetic and Yukawa interactions. Nevertheless, gauge invariance may be recovered through the use of a full vertex function. This has been discussed for both QED4 [25] and QED3 [19]. For QED4, the authors in Ref. [26] have verified that the mass function is gauge invariant for a few different gauge parameters; see Fig. 06 in that reference. In particular, the results with the full vertex function are very close to the corresponding result in the Landau gauge within the rainbow approach, indicating the relevance of the ladder approximation.

It is an experimental challenge to generate a finite mass for massless Dirac particles in graphene. From the theoretical view, the task is to find a lesser critical coupling constant α_c, such that the electromagnetic interaction would be enough to generate a finite mass. Having that in mind, in two-dimensional materials, there exist several microscopic interactions, beyond the Coulomb repulsion. Hence, we believe our results are an encouraging step for deriving symmetry broken phases. Nevertheless, we have provided an analytical result for the mass function of a nonlocal model interacting with a four-fermion action. Several generalizations of this paper could be investigated, for instance, the role of an external magnetic field, the Fermi velocity, the chemical potential, and the finite temperature. Furthermore, we may generalize our four-fermion interaction to a Thirring version [20] or other important microscopic interaction. We shall study these cases elsewhere.

ACKNOWLEDGMENTS

This work was supported in part by CNPq (Brazil), CAPES (Brazil), and FAPERJ (Brazil).

APPENDIX A: WAVE FUNCTION RENORMALIZATION

In this Appendix, we derive the integral equation for the wave function renormalization $A(p)$, defined in Eq. (23). To do so, we multiply Eq. (20) by $\gamma^\mu p_\mu$. Thereafter, we calculate the traces over the Dirac matrices. They yield

$$A(p) = 1 + \frac{1}{N_f D p^2}\mathrm{Tr}[\Xi(p)\gamma^\alpha p_\alpha]. \tag{A1}$$

Using Eqs. (21), (22), and (23) in Eq. (A1), after calculating the trace over Dirac matrices, we find

$$A(p) = 1 + \frac{2\lambda}{N_f p^2}\int \frac{d^3k}{(2\pi)^3}\frac{A(k)G(q)}{A(k)^2k^2 + \Sigma^2(p)}\frac{(k\cdot q)(p\cdot q)}{q^2} + \frac{1}{N_f}\int \frac{d^3k}{(2\pi)^3}\frac{p\cdot k}{p^2}\frac{A(k)\Delta_\varphi(p-k)}{A^2(k)k^2 + \Sigma^2(k)}, \tag{A2}$$

where $G(q)$ and q are given by

$$q = p - k, \tag{A3}$$

and

$$G(q) = \frac{1}{\sqrt{q^2}(2 + \frac{\lambda D}{32})}. \tag{A4}$$

We can solve the angular integral in Eq. (A2) to obtain

$$A(p) = 1 - \frac{B_1}{p^3}\int_0^\infty dk \frac{kA(k)}{A^2(k)k^2 + \Sigma^2(p)}\mathcal{B}_1(k,p) + - \frac{B_2}{p^3}\int_0^\infty dk \frac{kA(k)}{A^2(k)k^2 + \Sigma^2(p)}\mathcal{B}_2(k,p), \tag{A5}$$

where

$$B_1 = \frac{2\lambda}{N_f}\frac{1}{16\pi^2}\frac{1}{(2 + \frac{\lambda D}{32})}, \tag{A6}$$

$$B_2 = \frac{1}{DN_f}\frac{1}{3\pi^3}, \tag{A7}$$

$$\mathcal{B}_1(k,p) = \frac{1}{3}(p+k)^3 - \frac{1}{3}|p-k|^3 + (p^2 - k^2) \times [(p-k)\mathrm{Sgn}(p+k) - (p+k)\mathrm{Sgn}(p-k)], \tag{A8}$$

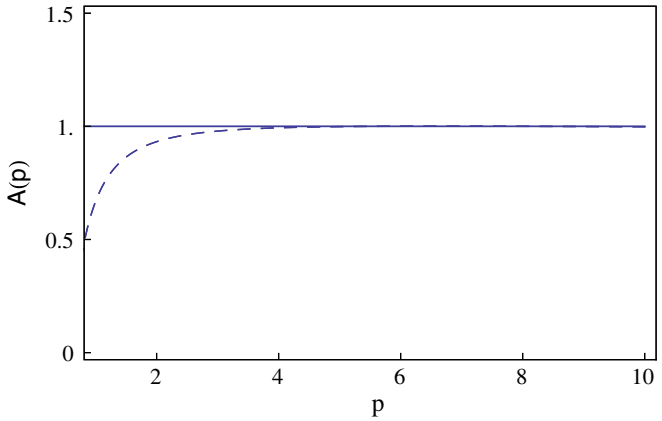

FIG. 2. Comparison between the numerical results of Eq. (A5) and the analytical solution $A(p) = 1.0$. The dashed line is the numerical solution with $\Sigma(p) = 0$ (symmetric phase). We choose $\alpha = 2.2$, $D = 4$, $N_f = 10$, $g = 0.1$, and $\Lambda = 10$ to perform the numerical calculations. The analytical approximation describes the numerical result well, in particular, for large momentum.

and

$$\begin{aligned}\mathcal{B}_2(k,p) = {} & [4k^2 + 4p^2 - 6(x_0 g)^{-2}](|p-k| - |p+k|) \\ & + 4kp[|p-k| + |p+k| - 3(x_0 g)^{-1}] \\ & - 6(x_0 g)^{-1}[k^2 + p^2 - (x_0 g)^{-2}] \\ & \times \ln\left[\frac{(x_0 g)^{-1} + |p-k|}{(x_0 g)^{-1} + |p+k|}\right]. \end{aligned} \tag{A9}$$

In Fig. 2, we compare the numerical results of this integral equation with the analytical solution $A(p) = 1$. As expected, a very good agreement is found at large momentum, which the integral equation may be solved.

APPENDIX B: ANALYTICAL APPROACH

To convert Eq. (31) into a differential equation, it is convenient to perform an approximation in the logarithmic kernel. In the lowest order, we have

$$\begin{aligned}\ln\left(\frac{x_0^{-1} + |x+y|}{x_0^{-1} + |x-y|}\right) \approx {} & \frac{2y}{x + x_0^{-1}}\Theta(x-y) \\ & + \frac{2x}{y + x_0^{-1}}\Theta(y-x). \end{aligned} \tag{B1}$$

Introducing an ultraviolet cutoff Λ, we find

$$\begin{aligned} f(x) = {} & \frac{2C_1}{x}\left[\int_0^x \frac{y^2 f(y)dy}{y^2 + f^2(y)} + x\int_x^{g\Lambda} \frac{y f(y)dy}{y^2 + f^2(y)}\right] \\ & + gC_2\left[\int_0^x \frac{y^2 f(y)dy}{y^2 + f^2(y)} \frac{2}{x(x + x_0^{-1})}\right. \\ & \left. + \int_x^{g\Lambda} \frac{y f(y)dy}{y^2 + f^2(y)} \frac{2}{(y + x_0^{-1})}\right]. \end{aligned} \tag{B2}$$

On general grounds, the derivative of an arbitrary function $F(p)$, given by

$$F(p) = \int_{v(p)}^{u(p)} dk \mathcal{K}(k,p), \tag{B3}$$

is

$$\begin{aligned}\frac{dF(p)}{dp} = {} & \int_{v(p)}^{u(p)} dk \frac{\partial \mathcal{K}(k,p)}{\partial p} + \frac{\partial u}{\partial p}\mathcal{K}(p,u(p)) \\ & - \frac{\partial v}{\partial p}\mathcal{K}(p,v(p)), \end{aligned} \tag{B4}$$

where $v(p)$ and $u(p)$ are also arbitrary functions. Using this in Eq. (B2), we find

$$\begin{aligned}\frac{df}{dx} = {} & -\frac{2C_1}{x^2}\int_0^x \frac{y^2 f(y)dy}{y^2 + f^2(y)} \\ & + gC_2 \frac{d}{dx}\left[\frac{2}{x(x + x_0^{-1})}\right]\int_0^x \frac{y^2 f(y)dy}{y^2 + f^2(y)}. \end{aligned} \tag{B5}$$

For practical reasons, we define

$$h^{-1}(x) = 1 - \frac{gC_2 x^2}{2C_1}\frac{d}{dx}\left[\frac{2}{x(x + x_0^{-1})}\right]. \tag{B6}$$

By deriving Eq. (B5), we find

$$\frac{d}{dx}\left[h(x)x^2\frac{df}{dx}\right] + \frac{N_c}{4N_f}\frac{x^2 f(x)}{x^2 + f^2(x)} = 0, \tag{B7}$$

where N_c is given by Eq. (33). Finally, we consider the linearized version of Eq. (B5) with $x \gg f(x)$. In this case, the C_1-proportional term yields Eq. (32) with

$$\lim_{x \to g\Lambda}\left(x\frac{df(x)}{dx} + f(x)\right) = 0, \tag{B8}$$

and

$$\lim_{x \to 0} x^2 \frac{df(x)}{dx} = 0, \tag{B9}$$

representing the UV and IR asymptotic conditions, respectively.

APPENDIX C: COMPARISON BETWEEN NUMERICAL AND ANALYTICAL RESULTS

In this Appendix, we perform some numerical tests to verify the validity of the analytical approaches adopted in this paper. To obtain the numerical results for the mass function, we consider the full integral equation

for $\Sigma(p)$ with $A(p) = 1$, given by Eq. (28). The numerical result in Fig. 3 is obtained after we convert the momentum-dependent kernel in Eq. (28) into a system of nonlinear algebraic equations, using the repeated trapezoidal quadrature rule. Furthermore, it is mandatory to include a cutoff Λ to perform numerical calculations. Without loss of generality, we take $\Lambda = 10$ (in units of energy). For more details about these steps, see Ref. [7], which has this procedure for PQED at zero temperature and Ref. [8] at finite temperature.

The analytical solution $\Sigma(p)$ is promptly obtained from Eq. (35). Indeed, it has been shown that $\Sigma(p) = g^{-1}f(gp)$ in Sec. VI. After we assume $A_+ + A_- = 2.7/350$ and $A_+ - A_- = i2.7/350$, a very good agreement is observed between numerical and analytical results; see Fig. 3. This assumption is possible because A_+ and A_- are arbitrary constants as we discussed in Sec. VI. Equation (41) yields the critical point. Using $D = 4$ and $N_f = 2.0$, we have $\alpha_c \approx 0.36$. By changing g from 0.1 to 10, we have verified that the mass function slowly varies, which indicate that the critical phase is only dependent on α, as expected. The numerical results are also in agreement with the fact that dynamical mass generation only occurs for $\alpha \geq \alpha_c$.

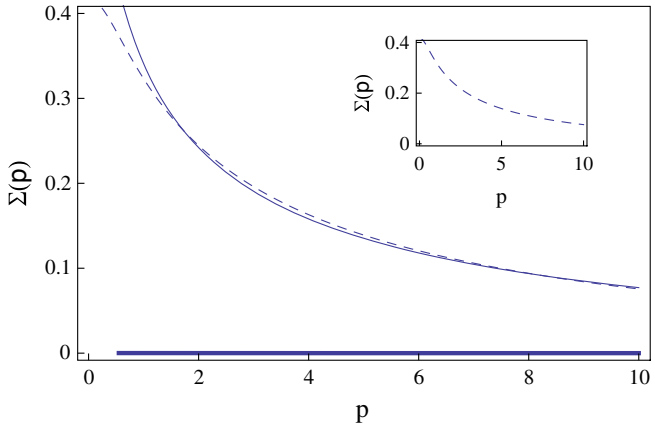

FIG. 3. Comparison between the numerical results of Eq. (28) and the analytical solution in Eq. (35). The common line is the analytical solution, the dashed line is the numerical result with $\alpha = 2.2$, and the thick line is the numerical result with $\alpha = 0.3$. We choose the parameters $\Lambda = 10$, $g = 0.1$, $D = 4$, and $N_f = 2.0$ for all the lines. The critical coupling constant is $\alpha_c = 0.36$, given by Eq. (41). For the analytical solution, we consider $A_+ + A_- = 2.7/350$ and $A_+ - A_- = i2.7/350$, the best fitting parameters. The inset is the numerical solution for $\alpha = 2.2$ to facilitate its visualization.

[1] A. H. Castro Neto, F. Guinea, N. M. R. Peres, K. S. Novoselov, and A. K. Geim, The electronic properties of graphene, Rev. Mod. Phys. **81**, 109 (2009).

[2] C. D. Roberts and A. G. Williams, Dyson-Schwinger equations and their application to hadronic physics, Prog. Part. Nucl. Phys. **33**, 477 (1994).

[3] D. J. Thouless, M. Kohmoto, M. P. Nightingale, and M. den Nijs, Quantized Hall Conductance in a Two-Dimensional Periodic Potential, Phys. Rev. Lett. **49**, 405 (1982).

[4] F. D. M. Haldane, Model for a Quantum Hall Effect without Landau Levels: Condensed-Matter Realization of the "Parity Anomaly", Phys. Rev. Lett. **61**, 2015 (1988).

[5] E. C. Marino, Quantum electrodynamics of particles on a plane and the Chern-Simons theory, Nucl. Phys. **B408**, 551 (1993).

[6] E. C. Marino, L. O. Nascimento, V. S. Alves, and C. M. Smith, Interaction induced quantum valley Hall effect in graphene, Phys. Rev. X **5**, 011040 (2015).

[7] V. S. Alves, W. S. Elias, L. O. Nascimento, V. Juričić, and F. Peña, Chiral symmetry breaking in the pseudoquantum electrodynamics, Phys. Rev. D **87**, 125002 (2013).

[8] L. O. Nascimento, V. S. Alves, F. Peña, C. M. Smith, and E. C. Marino, Chiral-symmetry breaking in pseudoquantum electrodynamics at finite temperature, Phys. Rev. D **92**, 025018 (2015).

[9] S. Teber, Electromagnetic current correlations in reduced quantum electrodynamics, Phys. Rev. D **86**, 025005 (2012); Two-loop fermion self-energy and propagator in reduced QED$_{3,2}$, Phys. Rev. D **89**, 067702 (2014); A. V. Kotikov and S. Teber, Two-loop fermion self-energy in reduced quantum electrodynamics and application to the ultrarelativistic limit of graphene, Phys. Rev. D **89**, 065038 (2014); S. Teber and A. V. Kotikov, Interaction corrections to the minimal conductivity of graphene via dimensional regularization, Eur. Phys. J. Spec. Top. **107**, 57001 (2014).

[10] E. C. Marino, Complete bosonization of the Dirac fermion field in $2+1$ dimensions, Phys. Lett. B **263**, 63 (1991).

[11] E. C. Marino, L. O. Nascimento, V. Sérgio Alves, and C. Morais Smith, Unitarity of theories containing fractional powers of the d'Alembertian operator, Phys. Rev. D **90**, 105003 (2014).

[12] A. Kovner and B. Rosenstein, Kosterlitz-Thouless mechanism of two-dimensional superconductivity, Phys. Rev. B **42**, 4748 (1990); N. Dorey and N. E. Mavromatos, QED$_3$ and two-dimensional superconductivity without parity violation, Nucl. Phys. **B386**, 614 (1992).

[13] R. L. P. G. do Amaral and E. C. Marino, Canonical quantization of theories containing fractional powers of the d'Alembertian operator, J. Phys. A **25**, 5183 (1992).

[14] M. A. H. Vozmediano and F. Guinea, Effect of Coulomb interactions on the physical observables of graphene, Phys. Scr. T **T146**, 014015 (2012); F. de Juan, A. G. Grushin, and M. A. H. Vozmediano, Renormalization of Coulomb interaction in graphene: Determining observable quantities, Phys. Rev. B **82**, 125409 (2010).

[15] D. C. Elias, R. V. Gorbachev, A. S. Mayorov, S. V. Morozov, A. A. Zhukov, P. Blake, L. A. Ponomarenko, I. V. Grigorieva, K. S. Novoselov, F. Guinea, and A. K. Geim, Dirac cones reshaped by interaction effects in suspended graphene, Nat. Phys. **7**, 701 (2011).

[16] L. O. Nascimento, Introduction to topological phases and electronic interactions in $(2+1)$ dimensions, Braz. J. Phys. **47**, 215 (2017).

[17] L. O. Nascimento, E. C. Marino, V. S. Alves, and C. M. Smith, Emerging Quantum Hall Effect in Massive Dirac Systems, arXiv: 1702.01573.

[18] T. Appelquist, M. J. Bowick, E. Cohler, and L. C. R. Wijewardhana, Chiral-Symmetry Breaking $2+1$ Dimensions, Phys. Rev. Lett. **55**, 1715 (1985).

[19] P. Maris, Influence of the full vertex and vacuum polarization on the fermion propagator in $(2+1)$-dimensional QED, Phys. Rev. D **54**, 4049 (1996).

[20] D. K. Hong and S. H. Park, Large-N analysis of the $(2+1)$-dimensional Thirring model, Phys. Rev. D **49**, 5507 (1994); V. A. Miransky and K. Yamawaki, On gauge theories with additional four-fermion interaction, Mod. Phys. Lett. A **04**, 129 (1989).

[21] D. J. Gross and A. Neveu, Dynamical symmetry breaking in asymptotically free field theories, Phys. Rev. D **10**, 3235 (1974).

[22] A. Coste and M. Luscher, Parity anomaly and fermion-boson transmutation in 3-dimensional lattice QED, Nucl. Phys. **B323**, 631 (1989).

[23] B. A. Bernevig with T. Hughes, *Topological Insulators and Topological Superconductors* (Princeton University, Princeton, NJ, 2013); S.-Q. Shen, Topological Insulators Dirac Equation in Condensed Matter, *Springer Series in Solid-State Sciences*, (Springer, Berlin, 2012); M. Z. Hasan and C. L. Kane, Colloquium: Topological insulators, Rev. Mod. Phys. **82**, 3045 (2010).

[24] K. Sasaki and R. Saito, Pseudospin and deformation-induced gauge field in graphene, Prog. Theor. Phys. Suppl. **176**, 253 (2008).

[25] D. Atkinson, J. C. R. Bloch, V. P. Gusynin, M. R. Pennington, and M. Reenders, Critical coupling in strong QED with weak gauge dependence, Phys. Lett. B **329**, 117 (1994).

[26] D. C. Curtis and M. R. Pennington, Nonperturbative study of the fermion propagator in quenched QED in covariant gauges using a renormalizable truncation of the Schwinger-Dyson equation, Phys. Rev. Abs. **48**, 4933 (1993).